



Analytic continuations of the Horn H_1 and H_5 functions

Souvik Bera^a and Tanay Pathak^b

Centre for High Energy Physics, Indian Institute of Science, Bangalore, Karnataka 560012, India

Received 30 June 2023 / Accepted 5 September 2023

© The Author(s), under exclusive licence to EDP Sciences, Springer-Verlag GmbH Germany, part of Springer Nature 2023

Abstract The analytic continuations (ACs) of the double variable Horn H_1 and H_5 functions have been derived for the first time using the automated symbolic *Mathematica* package `Olsson.w1`. The use of Pfaff–Euler transformations have been emphasised in deriving AC to cover regions which are otherwise not possible. The corresponding regions of convergence (ROC) are obtained using its companion package `ROC2.w1`. A *Mathematica* package `HornH1H5.w1`, containing all the derived ACs and the associated ROCs, along with a demonstration file of the same is made publicly available in this URL: https://github.com/souvik5151/Horn_H1_H5.git.

1 Introduction

Feynman integrals are an integral part of the precision calculations in quantum field theory [1]. They occur in the higher-order terms of the perturbation theory. Apart from this, they are also interesting from a mathematical point of view. Interest in Feynman integrals has also been motivated by processes at the LHC. In this quest to obtain the analytic properties, it was observed that hypergeometric functions and Feynman integrals are intimately related [2]. There are various ways to obtain and explore these hypergeometric connections of Feynman integrals. A general technique to evaluate these Feynman integrals, thus giving rise to multi-variable hypergeometric functions (MHFs), is that of using the Mellin–Barnes (MB) representation. Some of the classic results using it are results for general N -point one loop integrals [3–5]. Such evaluations give rise to the N -variable hypergeometric function of the Horn type. On the same front, a recently developed method of conic hull Mellin–Barnes (CHMB) [6–9], a generalised technique for finding the series representation of N -fold MB integrals, also gives a solution of Feynman integrals in terms of MHFs. Another method which achieves the same, and can be shown to be equivalent to the MB method, is that of the negative dimensional integration method [10–16]. In some cases, the hypergeometric representation of Feynman integrals can be obtained using the integration of the Feynman parametric integral [17–25] and without the use of any other specialised techniques. Recently, functional relations were used to evaluate one-loop Feynman integrals (see [26] and references within) in terms of MHFs. Feynman integrals can also be realised as the GKZ hypergeometric system [27–29]. These MHFs also appear in some physical processes too like Appell F_3 that appears in the calculation of one loop four-photon scattering amplitude [30, 31]. Apart from this, the evaluation of the pentagon integral [32] in certain Regge limit gives rise to Appell F_4 and Kampé de Fériet functions. To give a few more examples, two-loop massive sunset diagram [33, 34], three-loop vacuum diagram [24], one-loop two, three and four-point scalar functions [22, 35, 36] are also evaluated in terms of MHFs.

The theory of hypergeometric functions and their analytic continuations (ACs) in one and more than one variable is now a highly explored subject for over a century and is of fundamental importance in many branches of mathematical physics [37–43]. The one variable Gauss ${}_2F_1$ function has been generalised to two variables in [44], which are now known as Appell F_1 , F_2 , F_3 and F_4 functions. Another ten double variable hypergeometric functions G_1 , G_2 , G_3 and H_1 , H_2 , \dots , H_7 are introduced by Horn [45]. These 14 Appell–Horn functions form the set of distinct, second-order complete hypergeometric functions in two variables. More general higher-order functions, namely the Kampé de Fériet functions, frequently appear in the study of analytic continuations of these functions [38]. Using the detailed transformation theory of two-variable hypergeometric functions, it was found by Erdélyi [46] that all the second-order, two-variable hypergeometric functions, except F_4 , H_1 and H_5 , can be

^a e-mail: souvikbera@iisc.ac.in

^b e-mail: tanaypathak@iisc.ac.in (corresponding author)

related to F_2 via the transformation formulae. The Appell F_2 has been studied by Olsson [47] and recently have also been studied in [48], where a large number of ACs and their numerical implementation in *Mathematica* have been developed. The Appell F_4 was treated by Exton [49], and these results were further modified in [50]. It was also pointed out by Exton that H_1 and H_5 should be investigated in a similar way [49]. A recent study for the determination of the solution of the PDEs of various Appell and Horn functions along with that of H_1 and H_5 have been done in [51]. Some properties of the H_1 and H_5 have recently been studied in [52–56].

In all of the above examples, both mathematical and physical, it is thus important to obtain the ACs of the obtained MHFs. Mathematically, such ACs are important to obtain the solutions of the associated system of partial differential equations around various singular points. In physical applications, they are important so as to evaluate these functions in various kinematical regions. In [46], it was pointed out that the well-known transformation formulae of the one variable ${}_pF_{p-1}$ functions can be used to find the ACs of the MHFs. The method has been used for the Appell F_1 [57], F_4 [49] and recently for F_2 [48]. In principle, such computations are possible and have been achieved by hand before, but as we discuss below in the upcoming section, the analysis for the cases of H_1 and H_5 is tedious and demands the use of more powerful computational tools. Specifically one of the important steps in such analysis, the ROC analysis, is nearly impossible to do by hand. These occur due to the higher-order hypergeometric functions that appear in these studies.

With all the above motivation, in this work, we consider the non-trivial cases of Horn H_1 and H_5 series. Due to the difficulty in the computation of ACs and ROCs for these non-trivial cases, we use the automated *Mathematica* packages `Olsson.wl` and `ROC2.wl` [58], thus also aiming to test their efficacy. We aim to find the analytic continuations (ACs) of these so as to cover the whole real $x - y$ plane and their respective ROCs. We will also tacitly exclude the exceptional values of the parameters that are values that make the gamma functions that appear in the AC to be not defined. While deriving the ACs, we observe that only the use of AC of ${}_pF_{p-1}(z)$ around $z = \infty$ and the AC of ${}_2F_1(z)$ around $z = 1$, as has been done in a similar previous analysis of F_4 and F_2 , is no more adequate. To resolve this issue, we use the Pfaff–Euler transformations (PETs) of the ${}_2F_1$, wherever applicable, which allow us to cover the regions that are otherwise difficult to cover. For the case of H_1 , we found that such an approach allows us to cover the whole real plane, apart from some boundaries and singular points. On the other hand, for the Horn H_5 function, there still remains a small finite size region where no AC is valid (see Fig. 29). Since it is impossible to present all the results in the form of running text, we provide along with this manuscript a *Mathematica* [59] package and a demonstration file of the package. The package can be used to access the ACs and their corresponding ROCs as required by the user. However, we point out that special care has to be taken for the numerical evaluation, as the ACs can have multivaluedness issues which are not discussed in the present paper. These non-trivial evaluations are thus a challenge to the package in terms of both evaluating the analytic continuations for these two cases as well as finding the region of convergence for various higher-order series that appear in these analytic continuations. These results can further be used as a benchmark for future numerical tests of the same.

The scheme of this paper is as follows. In Sect. 2, we first analyzed H_1 , starting with the derivation of one of its simple ACs for the illustration. All the other ACs are derived using the package `Olsson.wl` that follows the same methodology. Similarly, we have discussed H_5 in Sect. 3. In all these sections, we discussed ways along with a road map to derive enough ACs that cover the whole real plane (boundaries excluded). We also illustrated the importance and uses of the Pfaff–Euler transformations of ${}_2F_1$ hypergeometric function during the process.

2 The Horn H_1 series

The Horn H_1 series is defined as [38, 45]

$$H_1(a, b, c, d, x, y) = \sum_{m, n=0}^{\infty} \frac{(a)_{m-n} (b)_{m+n} (c)_n x^m y^n}{m! n! (d)_m}, \quad (1)$$

with the ROC: $2\sqrt{|x||y|} + |y| < 1 \wedge |y| < 1 \wedge |x| < 1$, which for real x and y is shown in Fig. 1.

It satisfies the following system of partial differential equations:

$$\begin{aligned} x(1-x)r - y^2t + [d - (a+b+1)x]p - (a-b-1)yg - abz &= 0, \\ -y(1+y)t - x(1-y)s + [a-1 - (b+c+1)y]q - cyp - cbz &= 0, \end{aligned} \quad (2)$$

where the symbols are defined as follows:

$$z = H_1, \quad p = \frac{\partial z}{\partial x}, \quad q = \frac{\partial z}{\partial y},$$

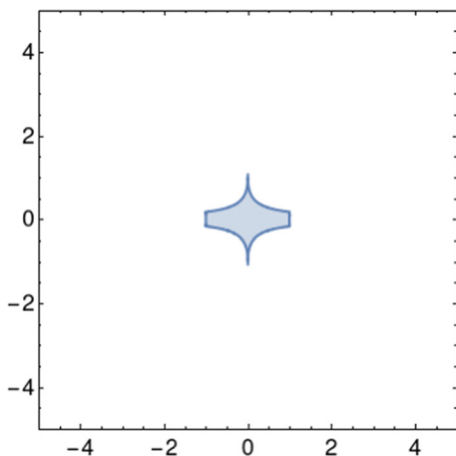


Fig. 1 ROC of Eq. (1)

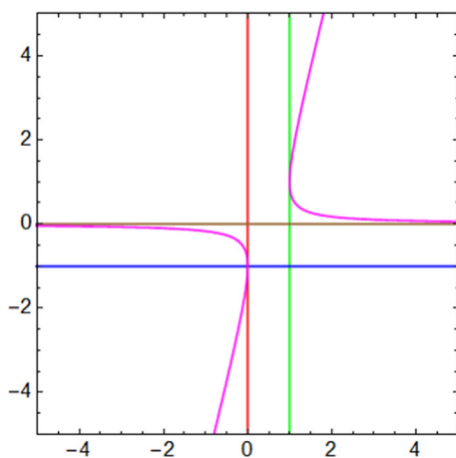


Fig. 2 Singular curve of H_1

$$r = \frac{\partial^2 z}{\partial x^2}, \quad t = \frac{\partial^2 z}{\partial y^2}, \quad s = \frac{\partial^2 z}{\partial x \partial y}.$$

The singular curves of the above equation are as follows; see Fig. 2.

$$x = 0, y = 0, x = 1, y = -1, -4xy + y^2 + 2y + 1 = 0. \tag{3}$$

In the following section, we obtain the various ACs of the H_1 series by using the ACs of ${}_pF_{p-1}$. These ACs ensure that we cover the whole real xy plane with the exception of certain singular lines; in other words, we can find the value of H_1 outside its ROC given as in Fig. 1. We also make use of the Pfaff–Euler transformations of ${}_2F_1$ in the intermediate steps and show how to obtain the various other ACs that could not be or are at times hard to obtain using just the ACs of ${}_pF_{p-1}$.

2.1 An illustrative example

As an illustrative example of the procedure of finding the ACs, by deriving one simple AC of H_1 , we will derive the AC around $(1, 0)$.

We take Eq. (1) and sum over m ,

$$H_1(a, b, c, d, x, y) = \sum_{m, n=0}^{\infty} \frac{(-1)^n y^n (b)_n (c)_n}{n! (1-a)_n} {}_2F_1(b+n, a-n; d; x). \tag{4}$$

Now using the AC of ${}_2F_1(x)$ around $x = 1$ Eq. (46), we find two series:

$$\begin{aligned}
 H_{(1,0)}^{(1)}(a, b, c, d, x, y) &= \frac{\Gamma(d)\Gamma(-a-b+d)}{\Gamma(d-a)\Gamma(d-b)} \sum_{m,n=0}^{\infty} \frac{y^n (b)_n (c)_n (b-d+1)_n}{n! (1-a)_n (d-a)_n} \\
 &\quad \times {}_2F_1(a-n, b+n; a+b-d+1; 1-x) \\
 &= \frac{\Gamma(d)\Gamma(-a-b+d)}{\Gamma(d-a)\Gamma(d-b)} \sum_{m,n} \frac{(c)_n (a)_{m-n} (b-d+1)_n (b)_{m+n}}{m! n! (d-a)_n (a+b-d+1)_m} (1-x)^m (-y)^n
 \end{aligned} \tag{5}$$

with ROC: $2\sqrt{|1-x||-y|} + |-y| < 1 \wedge |1-x| < 1 \wedge |-y| < 1$
 and

$$\begin{aligned}
 H_{(1,0)}^{(2)}(a, b, c, d, x, y) &= (1-x)^{-a-b+d} \frac{\Gamma(d)\Gamma(a+b-d)}{\Gamma(a)\Gamma(b)} \sum_{m,n=0}^{\infty} \frac{y^n (c)_n}{n!} \\
 &\quad \times {}_2F_1(-b+d-n, -a+d+n; -a-b+d+1; 1-x) \\
 &= (1-x)^{-a-b+d} \frac{\Gamma(d)\Gamma(a+b-d)}{\Gamma(a)\Gamma(b)} \\
 &\quad \sum_{m,n=0}^{\infty} \frac{(c)_n (b-d+1)_n (d-a)_{m+n} (d-b)_{m-n}}{m! n! (d-a)_n (-a-b+d+1)_m} (1-x)^m (-y)^n.
 \end{aligned} \tag{6}$$

So, we get the following AC around (1,0):

$$\begin{aligned}
 H_1(a, b, c, d, x, y) &= \frac{\Gamma(d)\Gamma(-a-b+d)}{\Gamma(d-a)\Gamma(d-b)} \sum_{m,n=0}^{\infty} \frac{(c)_n (a)_{m-n} (b-d+1)_n (b)_{m+n}}{m! n! (d-a)_n (a+b-d+1)_m} (1-x)^m (-y)^n + (1-x)^{-a-b+d} \\
 &\quad \times \frac{\Gamma(d)\Gamma(a+b-d)}{\Gamma(a)\Gamma(b)} \sum_{m,n=0}^{\infty} \frac{(c)_n (b-d+1)_n (d-a)_{m+n} (d-b)_{m-n}}{m! n! (d-a)_n (-a-b+d+1)_m} (1-x)^m (-y)^n
 \end{aligned} \tag{7}$$

with ROC: $2\sqrt{|1-x||-y|} + |-y| < 1 \wedge |1-x| < 1 \wedge |-y| < 1$ as shown in Fig. 3.

We observe from Fig. 3 that around the singular point (1, 0), one AC is enough to cover the space around it. However, there might arise a situation where this is not possible. For example for the other singular point (0, -1), where we need two ACs around that singular point.

The following diagram illustrates the possible chain of the process that can be used to derive both the ACs around the singular point (0, -1).

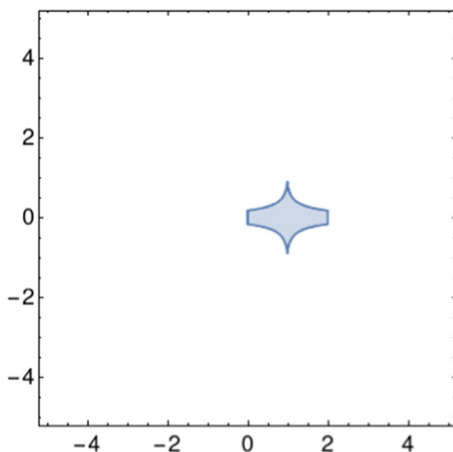


Fig. 3 ROC of Eq. (7)

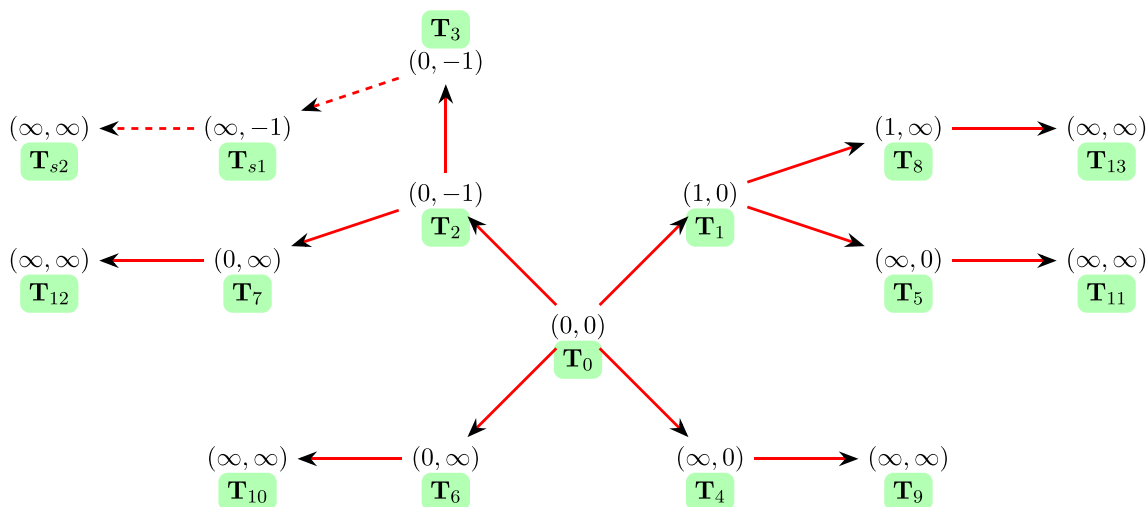
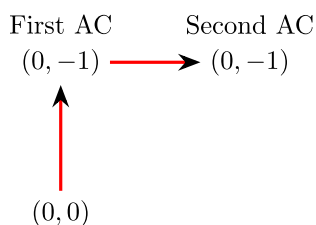
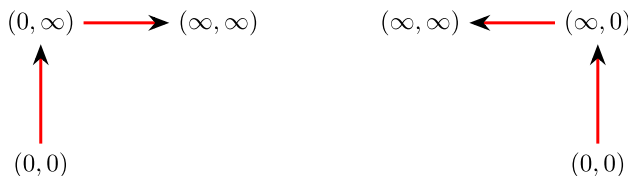


Fig. 4 All the possibilities of ACs for H_1 . The thick lines indicate the one that has been derived and the dashed lines denote which are not. The region that can be covered using the ACs denoted by dashed lines can be covered using the ACs denoted by the solid line. The derived ACs are part of the package and the AC T_i in the above graph is the i -th AC in the package



Using the AC of ${}_pF_{p-1}(z)$ around $z = \infty$, we have the following two possible situations:



Taking into account all these possibilities, we can have in general the following possibilities for H_1 (Fig. 4).

2.2 The Pfaff–Euler transformations

In the intermediate steps of the analytic continuation procedure, it is sometimes possible to get ${}_2F_1$ hypergeometric function when carrying out one of the summations. Instead of using the usual AC of ${}_2F_1(z)$ around $z = 1$ or $z = \infty$, it is also possible to use the PETs, Eq. (45), in the intermediate steps. This process can also be done using Olsson.wl. Using this we get the following transformations for H_1

We first take Eq. (1). Summing over m , we find

$$H_1(a, b, c, d, x, y) = \sum_{m,n=0}^{\infty} \frac{(-1)^n y^n (b)_n (c)_n}{n! (1-a)_n} {}_2F_1(b+n, a-n; d; x). \tag{8}$$

Now using the PETs of ${}_2F_1$, we find

$$H_1(a, b, c, d, x, y) = (1-x)^{-b} \sum_{m,n=0}^{\infty} \frac{(c)_n (b)_{m+n} (d-a)_{m+n}}{m! n! (1-a)_n (d)_m (d-a)_n} \left(\frac{x}{x-1}\right)^m \left(\frac{y}{x-1}\right)^n, \tag{9}$$

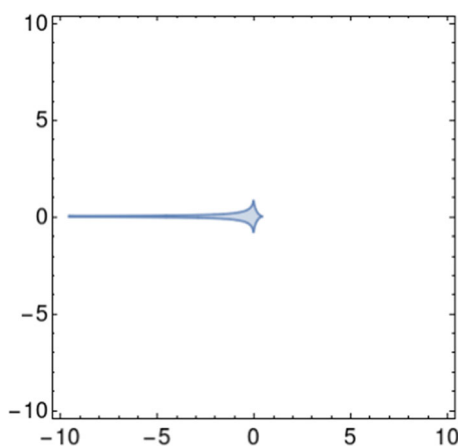


Fig. 5 ROC of Eq. (9)

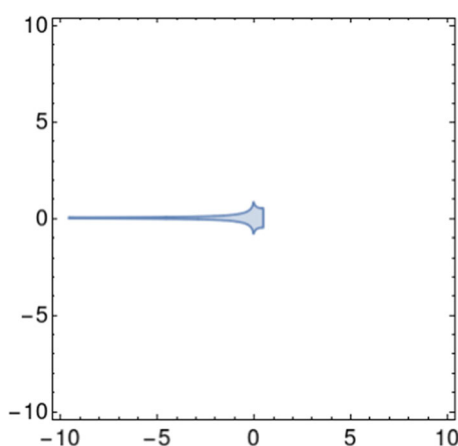


Fig. 6 ROC of Eq. (10)

with ROC: $\sqrt{\left|\frac{y}{x-1}\right|} + \sqrt{\left|\frac{x}{x-1}\right|} < 1$. (Figs. 5, 6)

$$H_1(a, b, c, d, x, y) = (1-x)^{-a} \sum_{m,n=0}^{\infty} \frac{(b)_n(c)_n(a)_{m-n}(b-d+1)_n(d-b)_{m-n}}{m!n!(d)_m} \left(\frac{x}{x-1}\right)^m (y(x-1))^n, \quad (10)$$

with ROC: $\sqrt{\left|\frac{x}{x-1}\right|} - \frac{1}{\sqrt{|y(x-1)|}} < -1 \wedge |y(x-1)| < 1 \wedge \left|\frac{x}{x-1}\right| < 1$.

$$H_1(a, b, c, d, x, y) = (1-x)^{-a-b+d} \sum_{m,n=0}^{\infty} \frac{(b)_n(c)_n(b-d+1)_n(d-a)_{m+n}(d-b)_{m-n}}{m!n!(1-a)_n(d)_m(d-a)_n} x^m y^n, \quad (11)$$

with the ROC same as H_1 : $2\sqrt{|x||y|} + |y| < 1 \wedge |y| < 1 \wedge |x| < 1$. (Figs. 7, 8)

Similarly, summing over n , we find

$$H_1(a, b, c, d, x, y) = \sum_{m,n=0}^{\infty} \frac{x^m(a)_m(b)_m}{m!(d)_m} {}_2F_1(c, b+m; -a-m+1; -y). \quad (12)$$

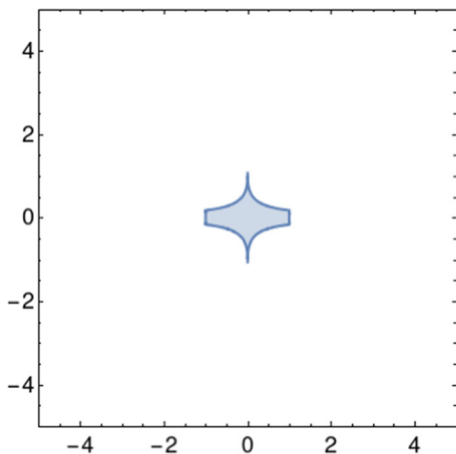


Fig. 7 ROC of Eq. (11)

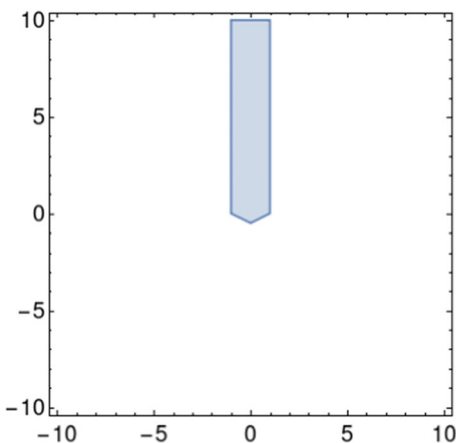


Fig. 8 ROC of Eq. (13)

Using PETs of ${}_2F_1$, we find:

$$H_1(a, b, c, d, x, y) = (y + 1)^{-b} \sum_{m, n=0}^{\infty} \frac{(a + c)_m (b)_{m+n} (-a - c + 1)_{n-m}}{m! n! (d)_m (1 - a)_{n-m}} \left(\frac{x}{y + 1}\right)^m \left(\frac{y}{y + 1}\right)^n, \quad (13)$$

with ROC $\left|\frac{x}{y+1}\right| + \left|\frac{y}{y+1}\right| < 1$.

$$H_1(a, b, c, d, x, y) = (y + 1)^{-c} \sum_{m, n=0}^{\infty} \frac{(b)_m (c)_n (a + b)_{2m} (-a - b + 1)_{n-2m}}{m! n! (d)_m (1 - a)_{n-m}} (-x)^m \left(\frac{y}{y + 1}\right)^n, \quad (14)$$

with ROC: $\frac{1}{|-x|} - 4 \left|\frac{y}{y+1}\right|^2 > 4 \left|\frac{y}{y+1}\right| \wedge |x| < 1 \wedge \left|\frac{y}{y+1}\right| < 1$.

$$H_1(a, b, c, d, x, y) = (y + 1)^{-a-b-c+1} \sum_{m, n=0}^{\infty} \frac{(b)_m (a + b)_{2m} (a + c)_m (-a - b + 1)_{n-2m} (-a - c + 1)_{n-m}}{m! n! (d)_m (1 - a)_{n-m}} \left(\frac{x}{(y + 1)^2}\right)^m (-y)^n, \quad (15)$$

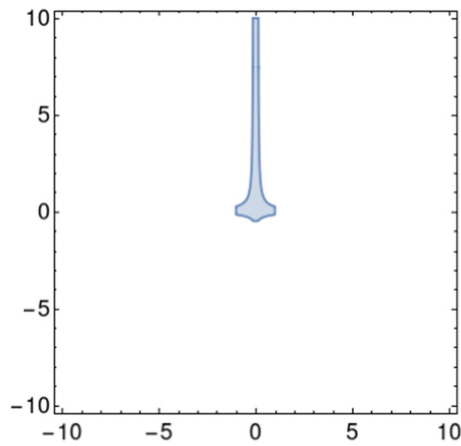


Fig. 9 The ROC of Eq. (14)

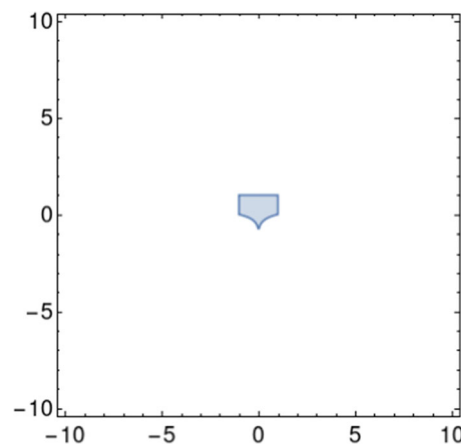


Fig. 10 The ROC of Eq. (15)

with ROC $\frac{1}{\sqrt{\left|\frac{x}{(y+1)^2}\right|}} - |-y| > 1 \wedge \left|\frac{x}{(y+1)^2}\right| < 1 \wedge |-y| < 1$. (Figs. 9, 10)

It is important to note that though the PETs have been used with the original definition of H_1 in the above case, one can also use them in the intermediate steps if summation over one of the indices gives ${}_2F_1$. AC number 22 (in the package) of H_1 is derived using this strategy.

One can then also use the whole procedure of finding the AC on the above-derived transformations of H_1 and obtain more ACs of H_1 . We derive AC number 20 and 21 (in the package) using this idea.

3 The Horn function H_5

The Horn function H_5 is defined as [37, 38, 45],

$$H_5 := H_5(a, b, c, x, y) = \sum_{m, n=0}^{\infty} \frac{(a)_{2m+n} (b)_{n-m} x^m y^n}{(c)_n m! n!}. \tag{16}$$

The defining ROC is given by [38]

$$|x| < \frac{1}{4} \wedge |y| < 1 \wedge,$$

$$|y| < \left(\begin{array}{l} \min \left(\frac{-(1-12|x|)^{3/2}+36|x|+1}{54|x|}, \frac{(1-12|x|)^{3/2}+36|x|+1}{54|x|}, \frac{(12|x|+1)^{3/2}-36|x|+1}{54|x|} \right) \sqrt{|x|} < \frac{1}{2\sqrt{3}} \\ \frac{(12|x|+1)^{3/2}-36|x|+1}{54|x|} \\ \text{True} \end{array} \right) \tag{17}$$

The ROC above is shown in Fig. 11 for real values of x and y .

The Horn H_5 function satisfies the following set of PDEs:

$$\begin{aligned} x(1+4x)r + (4x-1)ys + y^2t + ((4a+6)x-b+1)p + 2(a+1)yq + a(1+a)z &= 0 \\ (y-1)yt + xys - 2x^2r - (x(a-2b+2))p + (y(a+b+1)-c)q + abz &= 0, \end{aligned} \tag{18}$$

where like before the symbols p, q, r, t and s are given below:

$$\begin{aligned} z &= H_5, & p &= \frac{\partial z}{\partial x}, & q &= \frac{\partial z}{\partial y}, \\ r &= \frac{\partial^2 z}{\partial x^2}, & t &= \frac{\partial^2 z}{\partial y^2}, & s &= \frac{\partial^2 z}{\partial x \partial y}. \end{aligned}$$

It is to be noted that the PDE of H_5 given in the book [37] is not correct. This observation is also noted in [51]. It is worth mentioning that the singular locus of the H_5 can be found by using the theory of \mathcal{D} -modules and Gröbner basis (see [60] for an application to Lauricella F_C). Some properties of the Horn H_5 function are studied in [53].

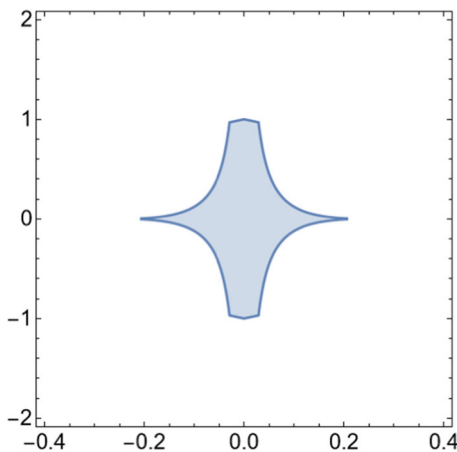


Fig. 11 The defining ROC of H_5 (Eq. (17)) is plotted for real values of x and y

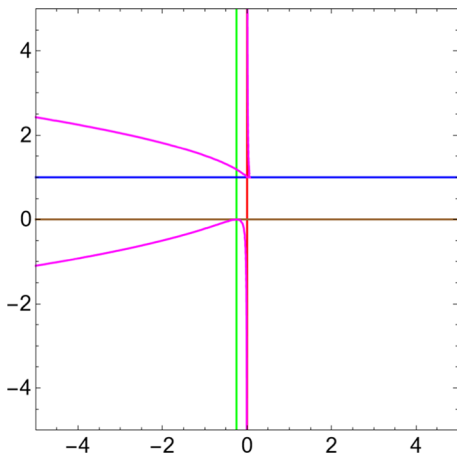


Fig. 12 The singular curves (i.e. Eq. (19)) are shown

The singular curves for the Horn H_5 are as follows:

$$x = 0, y = 0, x = -1/4, y = 1, \quad 1 + 8x + 16x^2 - y - 36xy + 27xy^2 = 0. \tag{19}$$

These are shown in Fig. 12.

In the following section, we find the ACs of the function using Olsson’s method. All the ACs are derived using the package `Olsson.wl` [58]. The ROCs of the ACs are obtained using the companion package `ROC2.wl`. The ROCs that are shown below are plotted for real values of x and y .

To proceed, we take the summation over the index m and observe that the Gauss ${}_2F_1$ appears inside the summand:

$$H_5(a, b, c, x, y) = \sum_{n=0}^{\infty} \frac{y^n (a)_n (b)_n}{n! (c)_n} {}_2F_1\left(\frac{a}{2} + \frac{n}{2}, \frac{a}{2} + \frac{n}{2} + \frac{1}{2}; -b - n + 1; -4x\right). \tag{20}$$

Similarly taking the summation over the index n , we find

$$H_5(a, b, c, x, y) = \sum_{m=0}^{\infty} \frac{(-1)^m x^m (a)_{2m}}{m! (1-b)_m} {}_2F_1(b - m, a + 2m; c; y). \tag{21}$$

The above two expressions (i.e. Eqs. (20) and (21)) are the starting points for our analysis of the H_5 function. Applying the well-known linear transformation formulae of Gauss ${}_2F_1$ listed in the Sect. 6.1, the ACs of H_5 can be found for general values of its Pochhammer parameters.

Let us take Eq. (21). Applying Eq. (46), we find the AC of H_5 around the point $(0, 1)$:

$$H_5 = \frac{\Gamma(c)\Gamma(-a-b+c)}{\Gamma(c-a)\Gamma(c-b)} \sum_{m,n=0}^{\infty} \frac{(a-c+1)_{2m} (a)_{2m+n} (b)_{n-m} (-x)^m (1-y)^n}{(c-b)_m (a+b-c+1)_{m+n} m! n!} + (1-y)^{-a-b+c} \frac{\Gamma(c)\Gamma(a+b-c)}{\Gamma(a)\Gamma(b)} \sum_{m,n=0}^{\infty} \frac{(a-c+1)_{2m} (c-a)_{n-2m} (c-b)_{m+n}}{m! n! (c-b)_m (-a-b+c+1)_{n-m}} \left(-\frac{x}{1-y}\right)^m (1-y)^n. \tag{22}$$

The first series of the above expression (Eq. (22)) is convergent in

$$|x| < \frac{1}{16} \wedge |1-y| < 1 \wedge |1-y| < \frac{(1-12|x|)^{3/2} - 18|x| + 1}{54|x|},$$

whereas the second series is valid for

$$\left| \frac{x}{y-1} \right| < 1 \wedge |1-y| < 1 \wedge |1-y| < \left(\begin{array}{l} \min\left(\frac{1}{27} \left(-\frac{(4|x|-3|y-1|)^{3/2}}{|\sqrt{x}(y-1)|} - \frac{8|x|}{|y-1|} + 9 \right), \frac{1}{27} \left(\frac{(4|x|+3|y-1|)^{3/2}}{|\sqrt{x}(y-1)|} - \frac{8|x|}{|y-1|} - 9 \right) \right) \quad 4 \left| \frac{x}{y-1} \right| > 3 \\ \frac{1}{27} \left(\frac{(4|x|+3|y-1|)^{3/2}}{|\sqrt{x}(y-1)|} - \frac{8|x|}{|y-1|} - 9 \right) \quad \text{True} \end{array} \right) \tag{23}$$

Hence, the AC (Eq. (22)) is valid in the common ROCs of the two series. We plot the ROCs of the individual series in Figs. 13 and 14.

We observe that the AC of H_5 in Eq. (22) does not cover the whole space around the singular point $(0, 1)$. Thus, we can find another AC that will cover the space that remains uncovered. To find such AC, we take the second series of Eq. (22) (let us denote it by S_2) and take the summation over m explicitly

$$S_2 = (1-y)^{-a-b+c} \frac{\Gamma(c)\Gamma(a+b-c)}{\Gamma(a)\Gamma(b)} \sum_{n=0}^{\infty} \frac{(1-y)^n (c-a)_n (c-b)_n}{n! (-a-b+c+1)_n} \times {}_4F_3\left(\frac{a}{2} - \frac{c}{2} + \frac{1}{2}, \frac{a}{2} - \frac{c}{2} + 1, a + b - c - n, -b + c + n; c - b, \frac{a}{2} - \frac{c}{2} - \frac{n}{2} + \frac{1}{2}, \frac{a}{2} - \frac{c}{2} - \frac{n}{2} + 1; \frac{x}{1-y}\right). \tag{24}$$

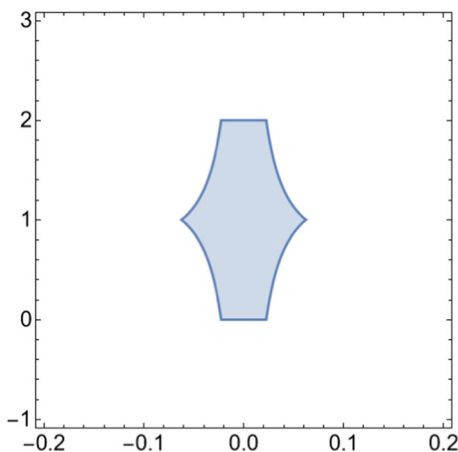


Fig. 13 The ROC of the first series of Eq. (22)

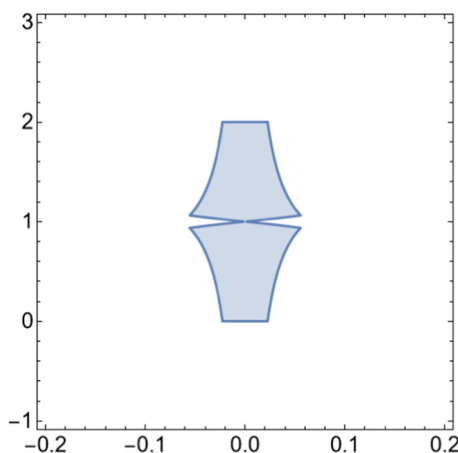


Fig. 14 The ROC of the second series of Eq. (22)

Now using the AC of ${}_4F_3(\dots; z)$ at $z = \infty$ (Eq. (49)), we find that only one series is non-vanishing. Denoting it as S'_2 ,

$$S'_2 = (1 - y)^{-a-b+c} \left(\frac{x}{y-1} \right)^{-a-b+c} \frac{\Gamma(c)\Gamma(a+b-c)}{\Gamma(a)\Gamma(b)} \sum_{m,n=0}^{\infty} \times \frac{(a+2b-2c+1)_{m-n}(a+b-c)_{m-n}(a+2b-c)_{2m-n}}{m!n!(a+2b-2c+1)_{m-2n}(a+2b-c)_{2(m-n)}} \left(\frac{1-y}{x} \right)^m (-x)^n, \tag{25}$$

whose ROC is given by

$$|r| < 1 \wedge \sqrt{|s|} < \min(z_1, z_2, z_3) \wedge |s| < \frac{1}{16}, \tag{26}$$

where $r = \frac{1-y}{x}$, $s = -x$ and

$$\begin{aligned} z_1 &= \text{second root of } 27z^4|r|^2 - 2z^2(9|r|+8) - |r|-1 = 0, \\ z_2 &= \text{second root of } 27z^4|r|^2 + 2z^2(9|r|-8) + |r|-1 = 0, \\ z_3 &= \text{second root of } 27z^4|r|^2 + 2z^2(9|r|+8) - |r|-1 = 0. \end{aligned}$$

This ROC is plotted in Fig. 15.

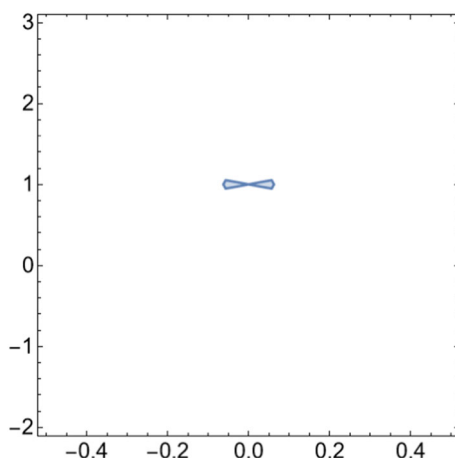


Fig. 15 The ROC of series S'_2 (i.e. Eq. (26)) is plotted for real values of x and y

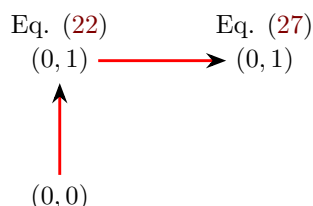


Fig. 16 The procedure to find the ACs around $(0, 1)$ is described as a directed graph

Hence, we find the second AC of H_5 around the point $(0, 1)$ by combining the first series of Eq. (22) with S'_2 (i.e. Eq. (25))

$$\begin{aligned}
 H_5 &= \frac{\Gamma(c)\Gamma(-a-b+c)}{\Gamma(c-a)\Gamma(c-b)} \sum_{m,n=0}^{\infty} \frac{(a-c+1)_{2m}(a)_{2m+n}(b)_{n-m}}{(c-b)_m(a+b-c+1)_{m+n}} \frac{(-x)^m(1-y)^n}{m!n!} + (1-y)^{-a-b+c} \left(\frac{x}{y-1}\right)^{-a-b+c} \\
 &\times \frac{\Gamma(c)\Gamma(a+b-c)}{\Gamma(a)\Gamma(b)} \sum_{m,n=0}^{\infty} \frac{(a+2b-2c+1)_{m-n}(a+b-c)_{m-n}(a+2b-c)_{2m-n}}{m!n!(a+2b-2c+1)_{m-2n}(a+2b-c)_{2(m-n)}} \left(\frac{1-y}{x}\right)^m (-x)^n. \quad (27)
 \end{aligned}$$

The ROC of this AC is the same as in Eq. (26), which is plotted in Fig. 15.

Let us summarise what we have achieved for H_5 so far. We started with the definition of the H_5 , whose ROC is given in Eq. (17) and plotted in Fig. 11. Taking summation over the index n yields the Gauss ${}_2F_1$ in the summand. Then good use of the AC of ${}_2F_1$ Eq. (46) is used to find the AC of H_5 at $(0, 1)$. The ROC of that AC is plotted in Fig. 14 for real values of x, y . Since the AC of H_5 around $(0, 1)$ does not cover the whole space around that point, we have derived another AC around the same point by transforming the second series of Eq. (22). The resultant AC is given in Eq. (27) and the ROC of it is plotted in Fig. 15. This procedure can be described by a directed graph as shown in Fig. 16, where the vertices represent the singular points and the directed edges denote the process of evaluation. We plot the ROCs of both the ACs around the point $(0, 1)$ along with the defining ROC of H_5 in Fig. 17.

We go on to derive the ACs of H_5 around $(0, \infty)$ and (∞, ∞) . The procedure is demonstrated via a directed graph in Fig. 18. To find the AC around $(0, \infty)$, we use Eq. (47) in Eq. (21) to find

$$\begin{aligned}
 H_5 &= (-y)^{-a} \frac{\Gamma(c)\Gamma(b-a)}{\Gamma(b)\Gamma(c-a)} \sum_{m,n=0}^{\infty} \frac{(a)_{2m+n}(a-c+1)_{2m+n}}{m!n!(a-b+1)_{3m+n}} \left(-\frac{x}{y^2}\right)^m \left(\frac{1}{y}\right)^n \\
 &+ (-y)^{-b} \frac{\Gamma(c)\Gamma(a-b)}{\Gamma(a)\Gamma(c-b)} \sum_{m,n=0}^{\infty} \frac{(b)_{n-m}(b-c+1)_{n-m}}{m!n!(-a+b+1)_{n-3m}} (-xy)^m \left(\frac{1}{y}\right)^n. \quad (28)
 \end{aligned}$$

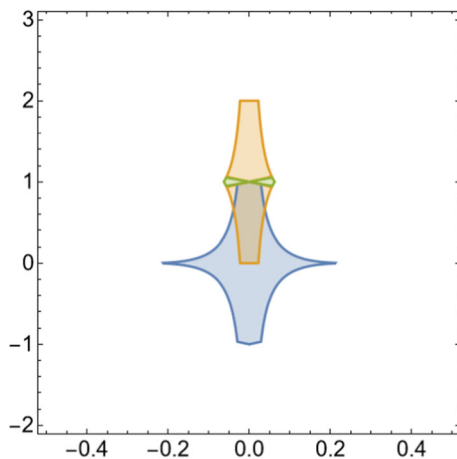


Fig. 17 The defining ROC of H_5 , the ROC of first AC around $(0, 1)$ (i.e. Eq. (22)) and the ROC of second AC around $(0, 1)$ (Eq. (27)) are plotted in blue, yellow and green, respectively, for real values of x, y

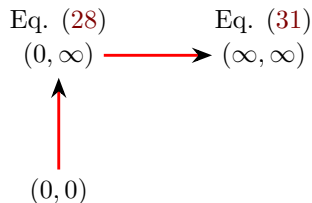


Fig. 18 The procedure to find the ACs around $(0, \text{inf})$ and (∞, ∞) are described as a directed graph

The ROC of the first series is given by

$$16 \left| \frac{x}{y^2} \right| < 27 \wedge \left| \frac{x}{y^2} \right| < \frac{1}{32} \left(\left(9 - \frac{8}{|y|} \right)^{3/2} - \frac{36}{|y|} + \frac{8}{|y|^2} + 27 \right) \wedge \frac{1}{|y|} < 1, \tag{29}$$

and the second series is valid in

$$27|xy| < 1 \wedge |y| < y^2 \wedge |xy| < \min \left(\frac{1}{32} \left(\left(9 - \frac{8}{|y|} \right)^{3/2} - \frac{36}{|y|} + \frac{8}{y^2} + 27 \right) |y|^3, \frac{1}{32} |y| \left(-\sqrt{|y|(9|y|+8)}^{3/2} + 36|y| + 27y^2 + 8 \right) \right). \tag{30}$$

These are plotted in Figs. 19 and 20, respectively. The ROC of the AC given in Eq. (28) is the intersection of the ROCs of both the series.

We observe that the second series can be transformed further to find the AC of H_5 around (∞, ∞) in a similar way to the second AC around $(0, 1)$. We find the AC around (∞, ∞) as

$$\begin{aligned}
 H_5 = & (-y)^{-a} \frac{\Gamma(c)\Gamma(b-a)}{\Gamma(b)\Gamma(c-a)} \sum_{m,n=0}^{\infty} \frac{(a)_{2m+n}(a-c+1)_{2m+n}}{m!n!(a-b+1)_{3m+n}} \left(-\frac{x}{y^2} \right)^m \left(\frac{1}{y} \right)^n \\
 & + (-y)^{-b} (-xy)^{\frac{b-a}{3}} \frac{\Gamma(1-b)\Gamma(c)\Gamma(\frac{a-b}{3})}{3\Gamma(a)\Gamma(-\frac{a}{3}-\frac{2b}{3}+1)\Gamma(-\frac{a}{3}+c-\frac{2b}{3})} \\
 & \times \sum_{m,n=0}^{\infty} \frac{(\frac{a-b}{3})_{m-\frac{n}{3}} (\frac{a}{3}+\frac{2b}{3})_{m+\frac{2n}{3}} (\frac{a}{3}+\frac{2b}{3}-c+1)_{m+\frac{2n}{3}} \left(\frac{1}{27xy} \right)^m \left(-\frac{\sqrt[3]{-xy}}{y} \right)^n}{m!n! \left(\frac{1}{3} \right)_m \left(\frac{2}{3} \right)_m \left(-\frac{a}{3}-\frac{2b}{3}+1 \right)_{-\frac{1}{3}(2n)} \left(\frac{a}{3}+\frac{2b}{3} \right)_{\frac{2n}{3}} \left(\frac{a}{3}+\frac{2b}{3}-c+1 \right)_{\frac{2n}{3}} \left(-\frac{a}{3}+c-\frac{2b}{3} \right)_{-\frac{2n}{3}}} \\
 & - \frac{2\pi 3^{-a+b-\frac{1}{2}} (-y)^{-b} \Gamma(1-b)\Gamma(c)\Gamma(a-b) (-xy)^{\frac{1}{3}(-a+b-1)}}{\Gamma(a)\Gamma(\frac{1}{3}(-a-2b+2))\Gamma(\frac{a-b}{3})\Gamma(\frac{1}{3}(a-b+2))\Gamma(\frac{1}{3}(-a-2b-1)+c)}
 \end{aligned}$$

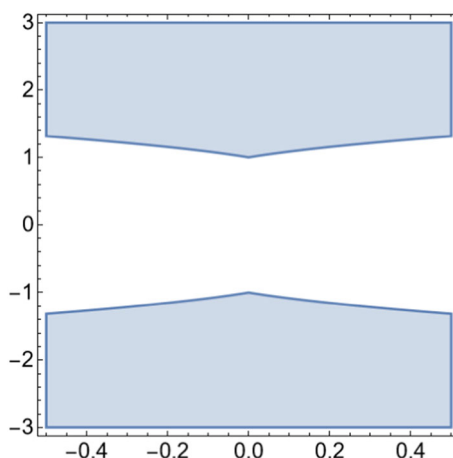


Fig. 19 The ROC of the first series of Eq. (28)

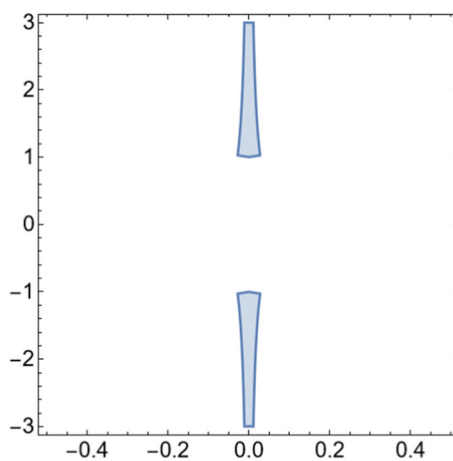


Fig. 20 The ROC of the second series of Eq. (28)

$$\begin{aligned}
 & \times \sum_{m,n=0}^{\infty} \frac{\left(\frac{a}{3} - \frac{b}{3} + \frac{1}{3}\right)_{m-\frac{n}{3}} \left(\frac{a}{3} + \frac{2b}{3} + \frac{1}{3}\right)_{m+\frac{2n}{3}} \left(\frac{a}{3} + \frac{2b}{3} - c + \frac{4}{3}\right)_{m+\frac{2n}{3}} \left(\frac{1}{27xy}\right)^m \left(-\frac{\sqrt[3]{-xy}}{y}\right)^n}{m! n! \left(\frac{2}{3}\right)_m \left(\frac{4}{3}\right)_m \left(-\frac{a}{3} - \frac{2b}{3} + \frac{2}{3}\right)_{-\frac{2n}{3}} \left(\frac{a}{3} + \frac{2b}{3} + \frac{1}{3}\right)_{\frac{2n}{3}} \left(\frac{a}{3} + \frac{2b}{3} - c + \frac{4}{3}\right)_{\frac{2n}{3}} \left(-\frac{a}{3} + c - \frac{2b}{3} - \frac{1}{3}\right)_{-\frac{2n}{3}}} \\
 & + \frac{\pi 3^{-a+b-\frac{1}{2}} (-y)^{-b} \Gamma(1-b) \Gamma(c) \Gamma(a-b) (-xy)^{\frac{1}{3}(-a+b-2)}}{\Gamma(a) \Gamma\left(\frac{1}{3}(-a-2b+1)\right) \Gamma\left(\frac{a-b}{3}\right) \Gamma\left(\frac{1}{3}(a-b+1)\right) \Gamma\left(-\frac{a}{3} + c - \frac{2(b+1)}{3}\right)} \\
 & \sum_{m,n=0}^{\infty} \frac{\left(\frac{a}{3} - \frac{b}{3} + \frac{2}{3}\right)_{m-\frac{n}{3}} \left(\frac{a}{3} + \frac{2b}{3} + \frac{2}{3}\right)_{m+\frac{2n}{3}} \left(\frac{a}{3} + \frac{2b}{3} - c + \frac{5}{3}\right)_{m+\frac{2n}{3}} \left(\frac{1}{27xy}\right)^m \left(-\frac{\sqrt[3]{-xy}}{y}\right)^n}{m! n! \left(\frac{4}{3}\right)_m \left(\frac{5}{3}\right)_m \left(-\frac{a}{3} - \frac{2b}{3} + \frac{1}{3}\right)_{-\frac{2n}{3}} \left(\frac{a}{3} + \frac{2b}{3} + \frac{2}{3}\right)_{\frac{2n}{3}} \left(\frac{a}{3} + \frac{2b}{3} - c + \frac{5}{3}\right)_{\frac{2n}{3}} \left(-\frac{a}{3} + c - \frac{2b}{3} - \frac{2}{3}\right)_{-\frac{2n}{3}}} \quad (31)
 \end{aligned}$$

We do not write the ROC of the above AC explicitly. It can be obtained from the ancillary file (See Sect. 6.3). The ROC is shown in Fig. 21.

To summarise, we have found four ACs of H_5 around the singular points $(0, 1)$, $(0, \infty)$ and (∞, ∞) . Two ACs are found around the neighbourhood of $(0, 1)$. The ROCs of these four ACs are plotted in Fig. 22. In an analogous way, starting from Eq. (20), one can find ACs around $(1, 0)$, which can further be used to find ACs around $(\infty, 0)$, $(1, \infty)$ and (∞, ∞) . The whole procedure of finding ACs of H_5 is demonstrated using the directed graph in Fig. 23. However finding all the ACs according to the graph is quite a laborious task in practice, due to the lengthy expressions of the ACs, even when one uses the computer program `Olsson.w1`.

On the other hand, one may use the PETs of the Gauss ${}_2F_1$ Eq. (45) to find some ACs of H_5 . We now show examples of how to find such ACs.

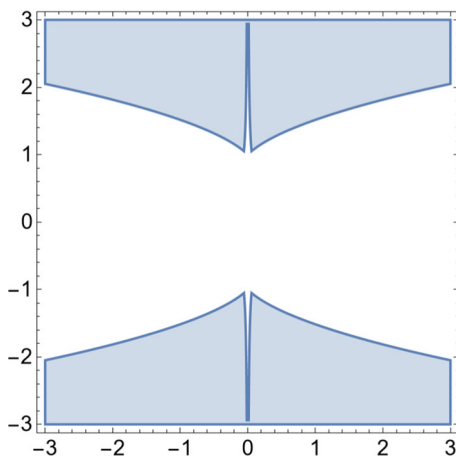


Fig. 21 The ROC of Eq. (31)

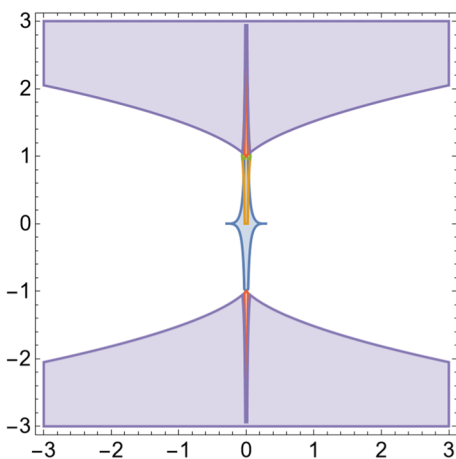


Fig. 22 The ROCs of the four ACs that are obtained so far

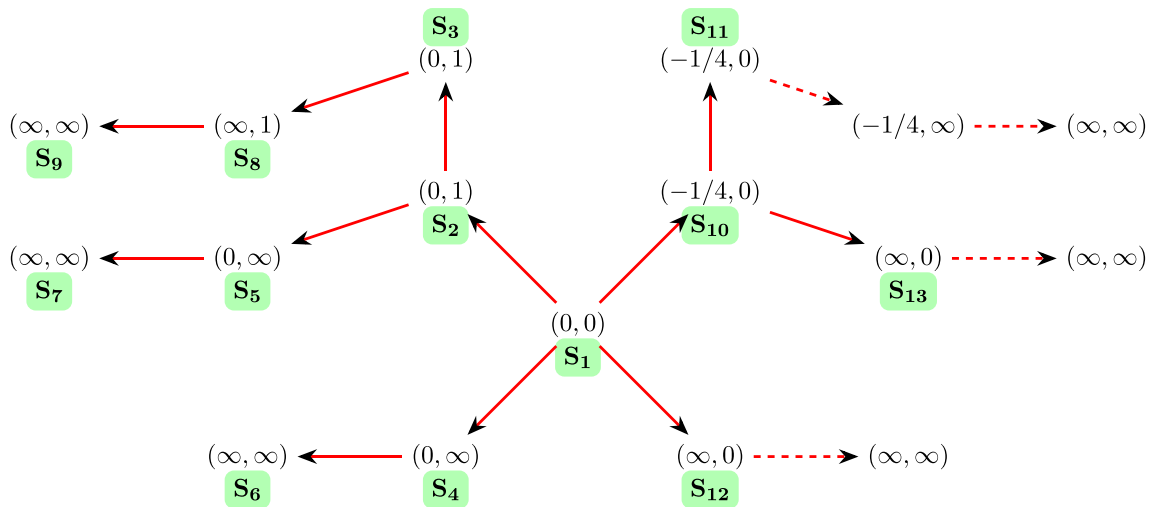


Fig. 23 The graph shows all the possibilities of obtaining ACs for H_5 . The thick lines indicates the ones that have been derived, and the dashed lines denote those which are not. The ROCs of the ACs that can be derived following the dashed lines overlap with the ROCs of the obtained 13 ACs. The other seven ACs that are not mentioned in the above graph are derived using the PETs of ${}_2F_1$

As before, our starting points are Eq. (20) and Eq. (21). Let us start with Eq. (20). Using the first PET (i.e. first equation of Eq. (45)), we find:

$$H_5 = (4x + 1)^{-\frac{a}{2}} \sum_{m,n=0}^{\infty} \frac{(a)_n \left(\frac{a}{2}\right)_{m+\frac{n}{2}} \left(\frac{1}{2}(-a - 2b + 1)\right)_{m-\frac{3n}{2}}}{m! n! \left(\frac{a}{2}\right)_{\frac{n}{2}} (c)_n \left(\frac{1}{2}(-a - 2b + 1)\right)_{-\frac{1}{2}(3n)} (1 - b)_{m-n}} \left(\frac{4x}{4x + 1}\right)^m \left(-\frac{y}{\sqrt{4x + 1}}\right)^n. \tag{32}$$

This AC is valid in

$$\left\{ |r| < 1 \wedge |s| < \frac{1}{4} \wedge |s| < \begin{pmatrix} \min(\Phi_1(r), \Phi_2(r), \Phi_3(r)) & |r| < \frac{1}{4} \\ \Phi_3(r) & \text{True} \end{pmatrix} \right\}, \tag{33}$$

where $r = \frac{4x}{4x+1}$, $s = -\frac{y^2}{16x+4}$. The functions $\Phi_i(r)$ are defined below:

$$\begin{aligned} \Phi_1(r) &= \frac{-128|r|^3 + 96|r|^2 + 3|r| - 2\sqrt{1 - |r|}\sqrt{-(4|r|-1)^3}(8|r|+1) + 2}{729|r|^2}, \\ \Phi_2(r) &= \frac{-128|r|^3 + 96|r|^2 + 3|r| + 2(8|r|+1)\sqrt{1 - |r|}\sqrt{-(4|r|-1)^3} + 2}{729|r|^2}, \\ \Phi_3(r) &= \frac{-2\sqrt{|r|+1}|1 - 8|r|| (4|r|+1)^{3/2} + 128|r|^3 + 96|r|^2 - 3|r| + 2}{729|r|^2}. \end{aligned} \tag{34}$$

Similarly using other two PETs, we find two more ACs. These are written below:

$$H_5 = (4x + 1)^{\frac{1}{2}(-a-1)} \sum_{m,n=0}^{\infty} \frac{(a)_n \left(\frac{a+1}{2}\right)_{m+\frac{n}{2}} \left(-\frac{a}{2} - b + 1\right)_{m-\frac{3n}{2}}}{m! n! \left(\frac{a+1}{2}\right)_{\frac{n}{2}} (c)_n \left(-\frac{a}{2} - b + 1\right)_{-\frac{1}{2}(3n)} (1 - b)_{m-n}} \left(\frac{4x}{4x + 1}\right)^m \left(-\frac{y}{\sqrt{4x + 1}}\right)^n. \tag{35}$$

We observe that the ROC of both the ACs Eqs. (32) and (35) are the same. Hence, the AC Eq. (35) is valid in the same ROC (i.e. Eq. (33)). The other AC can be found using the last PET (i.e. the last equation of Eq. (45):

$$H_5 = (4x + 1)^{-a-b+\frac{1}{2}} \sum_{m,n=0}^{\infty} \frac{(a)_n \left(\frac{1}{2}(-a - 2b + 1)\right)_{m-\frac{3n}{2}} \left(-\frac{a}{2} - b + 1\right)_{m-\frac{3n}{2}} (-4x)^m \left(-\frac{y}{(4x+1)^2}\right)^n}{m! n! (c)_n \left(\frac{1}{2}(-a - 2b + 1)\right)_{-\frac{1}{2}(3n)} \left(-\frac{a}{2} - b + 1\right)_{-\frac{1}{2}(3n)} (1 - b)_{m-n}} \tag{36}$$

$$|r| < 1 \wedge \sqrt{|s|} < \begin{pmatrix} \min(\Psi_1(r), \Psi_2(r), \Psi_3(r), \Psi_4(r)) \sqrt{|r|} < \frac{1}{\sqrt{3}} \\ \min(\Psi_3(r), \Psi_4(r)) & \text{True} \end{pmatrix} \wedge |s| < \frac{1}{4}, \tag{37}$$

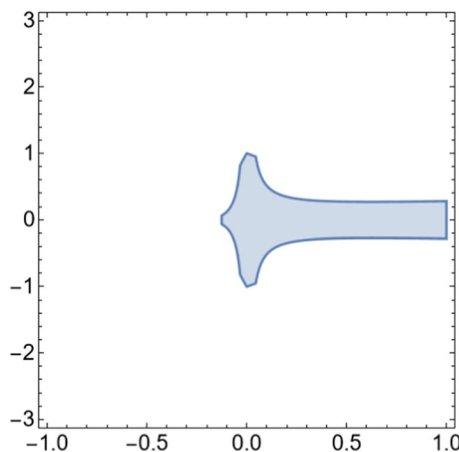


Fig. 24 The ROC of Eqs. (32) and (35)

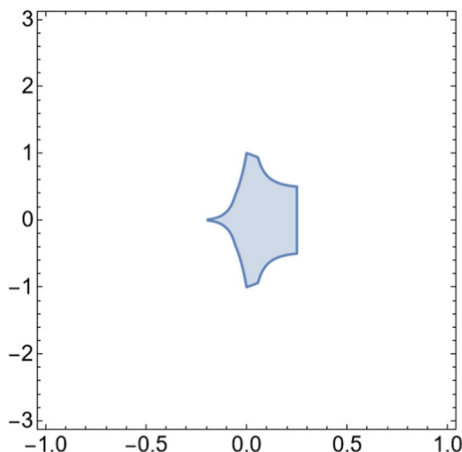


Fig. 25 The ROCs of Eq. (36)

where $r = -4x$, $s = \frac{y^2}{4(4x+1)^4}$. The functions $\Psi_i(r)$ are defined below:

$$\begin{aligned} \Psi_1(r) &= \frac{-(1 - 3|r|)^{3/2} + 9|r| + 1}{27(|r|^{3/2} + \sqrt{|r|})^2}, & \Psi_3(r) &= \frac{3|r|(\sqrt{3|r|+1} - 3) + \sqrt{3|r|+1} + 1}{27(|r|-1)^2|r|}, \\ \Psi_2(r) &= \frac{(1 - 3|r|)^{3/2} + 9|r| + 1}{27(|r|^{3/2} + \sqrt{|r|})^2}, & \Psi_4(r) &= \frac{\sqrt{3|r|+1} + 3|r|(\sqrt{3|r|+1} + 3) - 1}{27(|r|-1)^2|r|}. \end{aligned} \tag{38}$$

Starting with Eq. (21) and using three PETs, we find three ACs below:

$$H_5 = (1 - y)^{-b} \sum_{m,n=0}^{\infty} \frac{(a)_{2m}(a - c + 1)_{2m}(b)_{n-m}(c - a)_{n-2m}}{m!n!(c)_n} (x - xy)^m \left(\frac{y}{y - 1}\right)^n, \tag{39}$$

with ROC

$$\begin{aligned} &4|x - xy| < 1 \wedge \left|\frac{y}{y - 1}\right| < 1 \wedge \\ &|x - xy| < \frac{\sqrt{\left|\frac{y}{y-1}\right| + 8} \left|\frac{y}{y-1}\right|^{3/2} + \left|\frac{y}{y-1}\right|^2 - 20\left|\frac{y}{y-1}\right| + 8\sqrt{\left|\frac{y}{y-1}\right|} \sqrt{\left|\frac{y}{y-1}\right| + 8} - 8}{32\left(\left|\frac{y}{y-1}\right| - 1\right)^3} \end{aligned} \tag{40}$$

and

$$H_5 = (1 - y)^{-a} \sum_{m,n=0}^{\infty} \frac{(a)_{2m+n}(c - b)_{m+n}}{m!n!(1 - b)_m(c)_n(c - b)_m} \left(-\frac{x}{(y - 1)^2}\right)^m \left(\frac{y}{y - 1}\right)^n, \tag{41}$$

with ROC

$$4\left|\frac{x}{(y - 1)^2}\right| < 1 \wedge 32\left|\frac{x}{(y - 1)^2}\right| + \sqrt{\left|\frac{y}{y - 1}\right|} \left(\left|\frac{y}{y - 1}\right| + 8\right)^{3/2} + \left|\frac{y}{y - 1}\right|^2 < 20\left|\frac{y}{y - 1}\right| + 8 \wedge \left|\frac{y}{y - 1}\right| < 1 \tag{42}$$

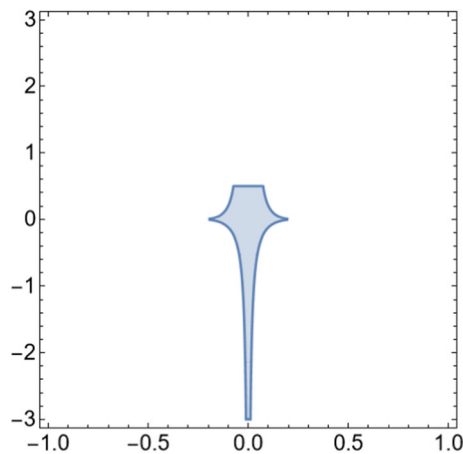


Fig. 26 The ROC of Eq. (39)

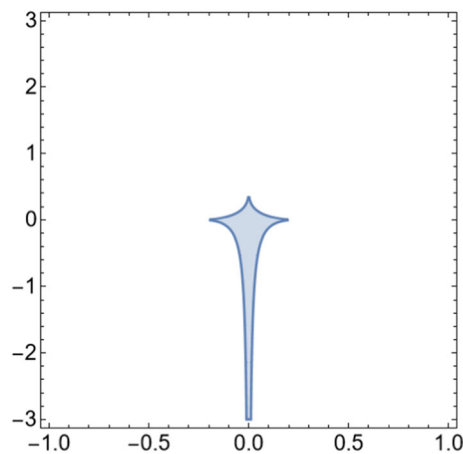


Fig. 27 The ROCs of Eq. (41)

and the last one

$$H_5 = (1 - y)^{-a-b+c} \sum_{m, n=0}^{\infty} \frac{(a)_{2m}(a - c + 1)_{2m}(c - a)_{n-2m}(c - b)_{m+n}}{m! n! (1 - b)_m (c)_n (c - b)_m} \left(\frac{x}{y - 1}\right)^m y^n, \tag{43}$$

with ROC

$$4 \left| \frac{x}{y - 1} \right| < 1 \wedge |y| < 1 \wedge \frac{\left(4 \left| \frac{x}{y - 1} \right| + 3\right)^{3/2}}{\sqrt{\left| \frac{x}{y - 1} \right|}} + 8 \left| \frac{x}{y - 1} \right| > 9(3|y| + 2). \tag{44}$$

All the ROCs of the six ACs are shown in Figs. 24, 25, 26, 27 and 28 for real values of x and y .

It is worth noting that the PETs of ${}_2F_1$ can be used in any intermediate step of the derivation, when the Gauss ${}_2F_1$ appears inside the summand, to find new ACs. We have applied it on the definition of the H_5 function only in this section to demonstrate the usefulness of the PETs of the Gauss ${}_2F_1$.

Even after analysing all the possible ways of applying the PETs in the intermediate steps of the derivation, we found no AC that is valid inside the small ‘white’ region as shown in Fig. 29.

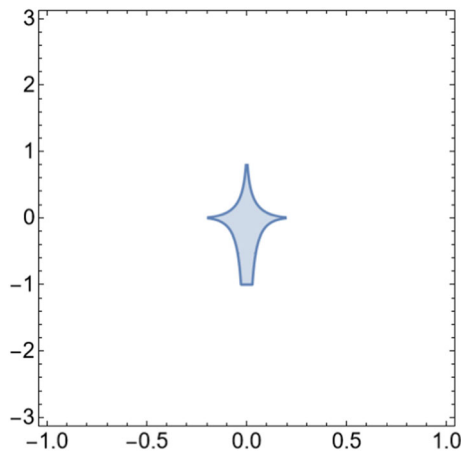


Fig. 28 The ROC of Eq. (43)

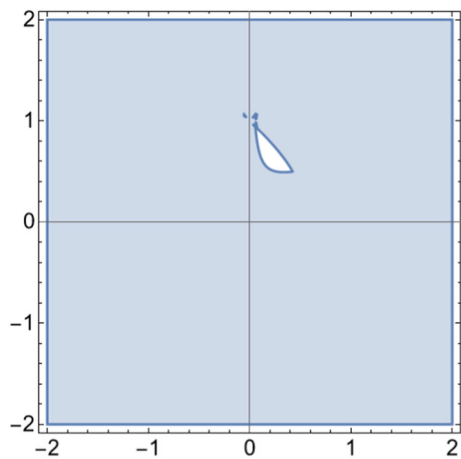


Fig. 29 The plot shows the uncovered region for real x, y

4 Summary

In this work, we have presented the various ACs and their corresponding ROCs of the Horn H_1 and H_5 functions. These results were derived using the publicly available *Mathematica* packages `Olsson.w1` and `ROC2.w1`. This ensures an easeful computation of the ACs and their ROCs which are otherwise prone to errors or difficult to compute by hand.

Our extensive work shows that the ACs of H_1 cover the whole real $x - y$ plane, with the exception of a few boundaries and singular lines, whereas the ACs of H_5 can be used to cover everywhere, except for the small region shown in Fig. 29. It is to be noted that in both cases, we are not able to give convergent expressions on the singular curves. It may be pointed out that the expressions given here have to be used carefully for numerical implementation due to the problem of multi-valuedness, which has not been discussed in this article. To this extent, it is the precise analogue of the work of Exton for Appell F_4 and Olsson for Appell F_1 . All the ACs derived here are valid for generic values of Pochhammer parameters. If the ACs are required to be used for the exceptional parameters, then one has to do the proper limiting procedure.

It is our view that investigations such as those reported here will go a long way in the advancements of the theory of hypergeometric functions, even for higher orders and higher numbers of variables, which in general are ubiquitous. Furthermore, the use of various symbolic computational packages used here makes them more significant for the analysis of complicated hypergeometric functions.

Acknowledgements The authors would like to thank B. Ananthanarayan for the discussions and comments on the draft. We also thank Samuel Friot for his continual encouragement and for having initiated us into this subject.

Data availability statement Data sharing is not applicable to this article as no datasets were generated or analysed during the current study.

Declarations

Conflict of interest We have no conflicts of interest to disclose.

Appendix

Appendix A

In this Appendix, we list some formulae that are used in deriving the ACs of the H_1 and H_5 functions.

- Euler transformation of ${}_2F_1$:

$$\begin{aligned} {}_2F_1(a, b, c; z) &= (1-z)^{-a} {}_2F_1\left(a, c-b, c, \frac{z}{z-1}\right) = (1-z)^{-b} {}_2F_1\left(c-a, b, c, \frac{z}{z-1}\right) \\ &= (1-z)^{c-a-b} {}_2F_1(c-a, c-b, c, z). \end{aligned} \quad (45)$$

- Analytic continuation of ${}_2F_1$ around $z = 1$:

$$\begin{aligned} {}_2F_1(a, b, c; z) &= \frac{\Gamma(c)\Gamma(c-a-b)}{\Gamma(c-a)\Gamma(c-b)} {}_2F_1(a, b, a+b-c+1; 1-z) + \frac{\Gamma(c)\Gamma(a+b-c)}{\Gamma(a)\Gamma(b)} (1-z)^{c-a-b} {}_2 \\ &\times F_1(c-a, c-b, c-a-b+1; 1-z). \end{aligned} \quad (46)$$

- Analytic continuation of ${}_2F_1$ around $z = \infty$:

$$\begin{aligned} {}_2F_1(a, b, c; z) &= \frac{\Gamma(c)\Gamma(b-a)}{\Gamma(b)\Gamma(c-a)} (-z)^{-a} {}_2F_1(a, a-c+1, a-b+1; \frac{1}{z}) \\ &+ \frac{\Gamma(c)\Gamma(a-b)}{\Gamma(a)\Gamma(c-b)} (-z)^{-b} {}_2F_1(b, b-c+1, b-a+1; \frac{1}{z}). \end{aligned} \quad (47)$$

- Analytic continuation of ${}_3F_2$ around $z = \infty$:

$$\begin{aligned} {}_3F_2\left(\begin{matrix} a_1, a_2, a_3 \\ b_1, b_2 \end{matrix} \middle| z\right) &= \frac{\Gamma(b_1)\Gamma(b_2)\Gamma(a_2-a_1)\Gamma(a_3-a_1)}{\Gamma(a_2)\Gamma(a_3)\Gamma(b_1-a_1)\Gamma(b_2-a_1)} (-z)^{-a_1} {}_3F_2\left(\begin{matrix} a_1, 1+a_1-b_1, 1+a_1-b_2 \\ 1+a_1-a_2, 1+a_1-a_3 \end{matrix} \middle| \frac{1}{z}\right) \\ &+ \frac{\Gamma(b_1)\Gamma(b_2)\Gamma(a_1-a_2)\Gamma(a_3-a_2)}{\Gamma(a_1)\Gamma(a_3)\Gamma(b_1-a_2)\Gamma(b_2-a_2)} (-z)^{-a_2} {}_3F_2\left(\begin{matrix} a_2, 1+a_2-b_1, 1+a_2-b_2 \\ 1+a_2-a_1, 1+a_2-a_3 \end{matrix} \middle| \frac{1}{z}\right) \\ &+ \frac{\Gamma(b_1)\Gamma(b_2)\Gamma(a_1-a_3)\Gamma(a_2-a_3)}{\Gamma(a_1)\Gamma(a_2)\Gamma(b_1-a_3)\Gamma(b_2-a_1)} (-z)^{-a_3} {}_3F_2\left(\begin{matrix} a_3, 1+a_3-b_1, 1+a_3-b_2 \\ 1+a_3-a_1, 1+a_3-a_2 \end{matrix} \middle| \frac{1}{z}\right). \end{aligned} \quad (48)$$

- Analytic continuation of ${}_4F_3$ around $z = \infty$:

$$\begin{aligned} {}_4F_3\left(\begin{matrix} a_1, a_2, a_3, a_4 \\ b_1, b_2, b_3 \end{matrix} \middle| z\right) &= \frac{\Gamma(b_1)\Gamma(b_2)\Gamma(b_3)\Gamma(a_2-a_1)\Gamma(a_3-a_1)\Gamma(a_4-a_1)}{\Gamma(a_2)\Gamma(a_3)\Gamma(a_4)\Gamma(b_1-a_1)\Gamma(b_2-a_1)\Gamma(b_3-a_1)} (-z)^{-a_1} \\ {}_4F_3\left(\begin{matrix} a_1, 1+a_1-b_1, 1+a_1-b_2, 1+a_1-b_3 \\ 1+a_1-a_2, 1+a_1-a_3, 1+a_1-a_4 \end{matrix} \middle| \frac{1}{z}\right) &+ \frac{\Gamma(b_1)\Gamma(b_2)\Gamma(b_3)\Gamma(a_1-a_2)\Gamma(a_3-a_2)\Gamma(a_4-a_2)}{\Gamma(a_1)\Gamma(a_3)\Gamma(a_4)\Gamma(b_1-a_2)\Gamma(b_2-a_2)\Gamma(b_3-a_2)} (-z)^{-a_2} \end{aligned}$$

$$\begin{aligned}
 & {}_4F_3 \left(\begin{matrix} a_2, 1+a_2-b_1, 1+a_2-b_2, 1+a_2-b_3 \\ 1+a_2-a_1, 1+a_2-a_3, 1+a_2-a_4 \end{matrix} \middle| \frac{1}{z} \right) + \frac{\Gamma(b_1)\Gamma(b_2)\Gamma(b_3)\Gamma(a_1-a_3)\Gamma(a_2-a_3)\Gamma(a_4-a_3)}{\Gamma(a_1)\Gamma(a_2)\Gamma(a_4)\Gamma(b_1-a_3)\Gamma(b_2-a_3)\Gamma(b_3-a_3)} (-z)^{-a_3} \\
 & {}_4F_3 \left(\begin{matrix} a_3, 1+a_3-b_1, 1+a_3-b_2, 1+a_3-b_3 \\ 1+a_3-a_1, 1+a_3-a_2, 1+a_3-a_4 \end{matrix} \middle| \frac{1}{z} \right) + \frac{\Gamma(b_1)\Gamma(b_2)\Gamma(b_3)\Gamma(a_1-a_4)\Gamma(a_2-a_4)\Gamma(a_3-a_4)}{\Gamma(a_1)\Gamma(a_2)\Gamma(a_3)\Gamma(b_1-a_4)\Gamma(b_2-a_4)\Gamma(b_3-a_4)} (-z)^{-a_4} \\
 & {}_4F_3 \left(\begin{matrix} a_4, 1+a_4-b_1, 1+a_4-b_2, 1+a_4-b_3 \\ 1+a_4-a_1, 1+a_4-a_2, 1+a_4-a_3 \end{matrix} \middle| \frac{1}{z} \right).
 \end{aligned} \tag{49}$$

- The analytic continuation around $z = \infty$ of ${}_pF_{p-1}(\dots; z)$ function can be found using the `Olsson.w1` package.

Appendix B

In this appendix, we give an outline of the various methods that are used to find the ROC of the hypergeometric series [38]. The methods are applicable to series with more than two variables as well. But the discussion below is focused on the double variable hypergeometric series and implemented in the companion package `ROC2.w1` of `Olsson.w1`:

1. **Cancellation of parameters:** Cancellation of parameters states that the region of convergence of a hypergeometric series is independent of the Pochhammer parameters. For example, consider the following Kampé de Fériet function:

$$S_1 = \sum_{m,n=0}^{\infty} \frac{(a)_{m+n}(b)_m(c)_n(d)_n}{(e)_m(f)_n(g)_n m! n!} x^m y^n. \tag{50}$$

Since the ROC is independent of the Pochhammer parameters, we can choose $d = g$, then the two Pochhammer symbols cancel and the series then effectively becomes similar to the Appell’s F_2 function and thus have the ROC: $|x|+|y| < 1$

2. **Horn’s theorem:** Horn’s theorem provides a more general way to find the ROC of a given hypergeometric series for any number of variables. The automatised implementation of the Horn’s theorem for two-variable hypergeometric series is performed in the package `ROC2.w1`. We will explain its working principle with an illustrative example below. Consider the following series:

$$S_2 = \sum_{m,n=0}^{\infty} \frac{(a)_{m+n}(b)_{m+n}(c)_m}{(d)_{2m+n} m! n!} X^m Y^n. \tag{51}$$

Writing the above series in a compact form:

$$S_2 = \sum_{m,n=0}^{\infty} A_{m,n} X^m Y^n. \tag{52}$$

We then evaluate the following two ratios:

$$f(m, n) = \frac{A_{m+1, n}}{A_{m, n}} = \frac{(a+m+n)(b+m+n)(c+m)}{(d+2m+n)(d+1+2m+n)(1+m)}, \tag{53}$$

$$g(m, n) = \frac{A_{m, n+1}}{A_{m, n}} = \frac{(a+m+n)(b+m+n)}{(d+2m+n)(1+n)}. \tag{54}$$

Now, we define two more functions as follows:

$$\begin{aligned}
 \Phi(\mu, \nu) &= \left| \lim_{t \rightarrow \infty} f(\mu t, \nu t) \right|^{-1}, \\
 \Psi(\mu, \nu) &= \left| \lim_{t \rightarrow \infty} g(\mu t, \nu t) \right|^{-1}.
 \end{aligned}$$

From this, one can construct the following two subsets of \mathbb{R}_+^2 :

$$C = \{(r, s) \mid 0 < r < \Phi(1, 0) \wedge 0 < s < \Psi(0, 1)\} \quad (55)$$

$$\doteq K[\Phi(1, 0), \Psi(0, 1)] \quad (56)$$

and

$$Z = \{(r, s) \mid \forall(m, n) \in \mathbb{R}_+^2 : 0 < r < \Phi(m, n) \wedge 0 < s < \Psi(m, n)\}. \quad (57)$$

The Horn's theorem for the two-variable hypergeometric functions is then given as follows.

Theorem 1 The union of $Z \cap C$ and its projections upon the co-ordinate axes is the representation in the absolute quadrant \mathbb{R}_+^2 of the region of convergence in \mathbb{C}^2 for the series F .

For S_2 , we then have

$$C = 0 < r < 4 \wedge 0 < s < 1$$

$$Z = r + s < 2s^{1/2}.$$

Using Horn's theorem, the ROC of the series S_2 is then given by

$$|x| < 4 \wedge |y| < 1 \wedge |x| + |y| < 2|y|^{1/2}. \quad (58)$$

Appendix C

In this appendix, we briefly describe the *Mathematica* [59] package `HornH1H5.wl` for the ease of the reader. Since it is not possible to present all the ACs of the Horn H_1 and H_5 function due to their lengthy expressions, we provide this package as an ancillary file. The package can be downloaded from the link below.

https://github.com/souvik5151/Horn_H1_H5.git

Once the file is downloaded, it can be called, after setting the correct path, as

```
In [] := <<HornH1H5.wl
```

This package can be used to access all the ACs as well as their corresponding ROCs. We have included the two commands for each of the function H_1 and H_5 in the package. These are the following:

1. `H1expose` and `H5expose`: These commands take an integer (less than the number of ACs) and give the output as a list of two elements containing the ROC and the expression of the AC, labelled by that number, of H_1 and H_5 , respectively. There are 22 ACs of H_1 and 20 ACs of H_5 .
2. `H1ROC` and `H5ROC`: These commands plot the ROC of a particular AC for real values of x and y , which is specified by a number given by the user, along with a user-specified point (x, y) . This command can be used when the user wants to determine if a certain point lies inside the ROC of an AC or not.

More information about these commands are available to the user via the `Information` command of *Mathematica* after loading the package.

References

1. S. Weinzierl, Feynman integrals. 2022. [arXiv:2201.03593](https://arxiv.org/abs/2201.03593) [hep-th]
2. M. Kalmykov, V. Bytev, B.A. Kniehl, S.-O. Moch, B.F.L. Ward, S.A. Yost, Hypergeometric Functions and Feynman diagrams. Antidifferentiation and the calculation of Feynman amplitudes. 2020. [arXiv:2012.14492](https://arxiv.org/abs/2012.14492) [hep-th]
3. A.I. Davydychev, Some exact results for N-point massive Feynman integrals. J. Math. Phys. **32**(4), 1052–1060 (1991)
4. A.I. Davydychev, General results for massive N-point Feynman diagrams with different masses. J. Math. Phys. **33**(1), 358–369 (1992)
5. E.E. Boos, A.I. Davydychev, A method of evaluating massive Feynman integrals. Theor. Math. Phys. **89**, 1052–1063 (1991)

6. B. Ananthanarayan, S. Banik, S. Friot, S. Ghosh, Multiple series representations of N-fold Mellin–Barnes integrals. *Phys. Rev. Lett.* **127**(15), 151601 (2021). [arXiv:2012.15108](#) [hep-th]
7. B. Ananthanarayan, S. Banik, S. Friot, S. Ghosh, Double box and hexagon conformal Feynman integrals. *Phys. Rev. D* **102**(9), 091901 (2020). [arXiv:2007.08360](#) [hep-th]
8. B. Ananthanarayan, S. Banik, S. Friot, S. Ghosh, Massive one-loop conformal Feynman integrals and quadratic transformations of multiple hypergeometric series. *Phys. Rev. D* **103**(9), 096008 (2021). [arXiv:2012.15646](#) [hep-th]
9. S. Banik, S. Friot, Multiple Mellin–Barnes integrals with straight contours. *Phys. Rev. D* **107**(1), 016007 (2023). [arXiv:2212.11839](#) [hep-ph]
10. I.G. Halliday, R.M. Ricotta, Negative dimensional integrals. 1. Feynman graphs. *Phys. Lett. B* **193**, 241–246 (1987)
11. A.T. Suzuki, E.S. Santos, A.G.M. Schmidt, One loop N point equivalence among negative dimensional, Mellin–Barnes and Feynman parametrization approaches to Feynman integrals. *J. Phys. A* **36**, 11859–11872 (2003). [arXiv:hep-ph/0309080](#)
12. D. Broadhurst, Two-loop negative-dimensional integration. *Phys. Lett. B* **197**(1), 179–182 (1987)
13. C. Anastasiou, E.W.N. Glover, C. Oleari, Application of the negative dimension approach to massless scalar box integrals. *Nucl. Phys. B* **565**, 445–467 (2000). [arXiv:hep-ph/9907523](#)
14. C. Anastasiou, E.W.N. Glover, C. Oleari, Scalar one loop integrals using the negative dimension approach. *Nucl. Phys. B* **572**, 307–360 (2000). [arXiv:hep-ph/9907494](#)
15. A.T. Suzuki, E.S. Santos, A.G.M. Schmidt, Massless and massive one loop three point functions in negative dimensional approach. *Eur. Phys. J. C* **26**, 125–137 (2002). [arXiv:hep-th/0205158](#)
16. A.T. Suzuki, E.S. Santos, A.G.M. Schmidt, General massive one loop off-shell three point functions. *J. Phys. A* **36**, 4465 (2003). [arXiv:hep-ph/0210148](#)
17. G. Somogyi, Angular integrals in d dimensions. *J. Math. Phys.* **52**, 083501 (2011). [arXiv:1101.3557](#) [hep-ph]
18. A.G. Grozin, A.V. Kotikov, HQET heavy-heavy vertex diagram with two velocities (2011). [arXiv:1106.3912](#) [hep-ph]
19. S. Abreu, R. Britto, H. Grönqvist, Cuts and coproducts of massive triangle diagrams. *JHEP* **07**, 111 (2015). [arXiv:1504.00206](#) [hep-th]
20. J. Ablinger, A. Behring, J. Blümlein, A. De Freitas, A. von Manteuffel, C. Schneider, Calculating three loop ladder and V-topologies for massive operator matrix elements by computer algebra. *Comput. Phys. Commun.* **202**, 33–112 (2016). [arXiv:1509.08324](#) [hep-ph]
21. T.-F. Feng, C.-H. Chang, J.-B. Chen, Z.-H. Gu, H.-B. Zhang, Evaluating Feynman integrals by the hypergeometry. *Nucl. Phys. B* **927**, 516–549 (2018). [arXiv:1706.08201](#) [hep-ph]
22. T.-F. Feng, C.-H. Chang, J.-B. Chen, H.-B. Zhang, The system of partial differential equations for the C0 function. *Nucl. Phys. B* **940**, 130–189 (2019). [arXiv:1809.00295](#) [hep-th]
23. X.-Y. Yang, H.-N. Li, The hypergeometric system for one-loop triangle integral. *Int. J. Mod. Phys. A* **34**(35), 1950232 (2020)
24. Z.-H. Gu, H.-B. Zhang, T.-F. Feng, Hypergeometric expression for a three-loop vacuum integral. *Int. J. Mod. Phys. A* **35**(19), 2050089 (2020)
25. A.G. Grozin, HQET vertex diagram: ϵ expansion. *Phys. Rev. D* **102**(5), 054022 (2020). [arXiv:2008.00342](#) [hep-ph]
26. O.V. Tarasov, Functional reduction of one-loop Feynman integrals with arbitrary masses. *JHEP* **06**, 155 (2022). [arXiv:2203.00143](#) [hep-ph]
27. L. de la Cruz, Feynman integrals as A-hypergeometric functions. *JHEP* **12**, 123 (2019). [arXiv:1907.00507](#) [math-ph]
28. R.P. Klausen, Hypergeometric series representations of Feynman integrals by GKZ hypergeometric systems. *JHEP* **04**, 121 (2020). [arXiv:1910.08651](#) [hep-th]
29. B. Ananthanarayan, S. Banik, S. Bera, S. Datta, FeynGKZ: A Mathematica package for solving Feynman integrals using GKZ hypergeometric systems. *Comput. Phys. Commun.* **287**, 108699 (2023). [arXiv:2211.01285](#) [hep-th]
30. O.V. Tarasov, Calculation of one-loop integrals for four-photon amplitudes by functional reduction method. (2022). [arXiv:2211.15535](#) [hep-ph]
31. A.I. Davydychev, Standard and hypergeometric representations for loop diagrams and the photon-photon scattering. in 7th International Seminar on High-energy Physics. (1993). [arXiv:hep-ph/9307323](#)
32. V. Del Duca, C. Duhr, E.W. Nigel Glover, V.A. Smirnov, The one-loop pentagon to higher orders in epsilon. *JHEP* **01**, 042 (2010). [arXiv:0905.0097](#) [hep-th]
33. F.A. Berends, M. Buza, M. Bohm, R. Scharf, Closed expressions for specific massive multiloop selfenergy integrals. *Z. Phys. C* **63**, 227–234 (1994)
34. B. Ananthanarayan, S. Friot, S. Ghosh, New series representations for the two-loop massive sunset diagram. *Eur. Phys. J. C* **80**(7), 606 (2020). [arXiv:1911.10096](#) [hep-ph]
35. T.-F. Feng, C.-H. Chang, J.-B. Chen, Z.-H. Gu, H.-B. Zhang, Evaluating Feynman integrals by the hypergeometry. *Nucl. Phys. B* **927**, 516–549 (2018). [arXiv:1706.08201](#) [hep-ph]
36. K.H. Phan, T. Riemann, Scalar 1-loop Feynman integrals as meromorphic functions in space-time dimension d. *Phys. Lett. B* **791**, 257–264 (2019). [arXiv:1812.10975](#) [hep-ph]
37. H. Bateman, *Higher Transcendental Functions* (McGraw-Hill Book Company, New York, 1953)
38. H.M. Srivastava, P.W. Karlsson, Multiple gaussian hypergeometric series (1985)
39. H. Exton, Multiple hypergeometric functions and applications (1976)
40. W.N. Bailey, *Cambridge Tracts in Mathematics and Mathematical Physics*, vol. 32 (University Press, 1935)

41. F.W.J. Olver, A.B. Olde Daalhuis, D.W. Lozier, B.I. Schneider, R.F. Boisvert, C.W. Clark, B.R. Miller, B.V. Saunders, H.S. Cohl, M.A. McClain (eds.), NIST Digital Library of mathematical functions. <http://dlmf.nist.gov/>. Release 1.1.7 of 2022-10-15
42. L. Slater, Generalized hypergeometric functions (1966)
43. K. Aomoto, M. Kita, Theory of Hypergeometric Functions. Springer Monographs in Mathematics (Berlin, 2011)
44. P. Appell, Sur les séries hypergéométriques de deux variables et sur des équations différentielles linéaires aux dérivés partielles, vol. 90 (French. C. R. Acad. Sci., Paris, 1880), pp. 296–299, 731–735
45. J. Horn, Hypergeometric functions of two variables. Math. Ann. **105**, 381–407 (1931)
46. A. Erdélyi, XXXIX—Transformations of hypergeometric functions of two variables. Proc. Roy. Soc. Edinb. Sect. A Math. Phys. Sci. **62**(3), 378–385 (1948)
47. P.O.M. Olsson, On the integration of the differential equations of five-parametric double-hypergeometric functions of second order. J. Math. Phys. **18**(6), 1285–1294 (1977). <https://doi.org/10.1063/1.523405>
48. B. Ananthanarayan, S. Bera, S. Friot, O. Marichev, T. Pathak, On the evaluation of the Appell F2 double hypergeometric function. (2021). [arXiv:2111.05798](https://arxiv.org/abs/2111.05798) [math.CA]
49. H. Exton, On the system of partial differential equations associated with Appell’s function F4. J. Phys. A Math. Gen. **28**(3), 631–641 (1995)
50. M. Huber, Infrared behavior of vertex functions in d-dimensional Yang–Mills theory. Other thesis (2007)
51. A. Debiard, B. Gaveau, Hypergeometric symbolic calculus. I—Systems of two symbolic hypergeometric equations. Bulletin des Sciences Mathématiques **126**(10), 773–829 (2002)
52. Y.A. Brychkov, N.V. Svischenko, On some formulas for the Horn functions $H_1(a, b, c; d; w, z)$ and $H(c) 1(a, b; d; w, z)$. Integral Transforms Spec. Funct. **32**(1), 31–47 (2021). <https://doi.org/10.1080/10652469.2020.1790554>
53. Y.A. Brychkov, N.V. Svischenko, On some formulas for the Horn functions $H_5(a, b; c; w, z)$ and $H(c) 5(a; c; w, z)$. Integral Transforms Spec. Funct. **33**(5), 373–387 (2022). <https://doi.org/10.1080/10652469.2021.1938026>
54. S.I. Bezrodnykh, Analytic continuation of the Horn hypergeometric series with an arbitrary number of variables. Integral Transforms Spec. Funct. **31**(10), 788–803 (2020). <https://doi.org/10.1080/10652469.2020.1744590>
55. A. Shehata, S.I. Moustafa, Some new formulas for the Horn’s hypergeometric functions. arXiv preprint [arXiv:2104.09140](https://arxiv.org/abs/2104.09140) (2021)
56. M. Pathan, A. Shehata, S.I. Moustafa, Certain new formulas for the Horn’s hypergeometric functions. Acta Universitatis Apulensis **64**(1), 137–170 (2020)
57. P.O.M. Olsson, Integration of the partial differential equations for the hypergeometric functions F1 and FD of two and more variables. J. Math. Phys. **5**(3), 420–430 (1964). <https://doi.org/10.1063/1.1704134>
58. B. Ananthanarayan, S. Bera, S. Friot, T. Pathak, Olsson.wl : a Mathematica package for the computation of linear transformations of multivariable hypergeometric functions. (2021). [arXiv:2201.01189](https://arxiv.org/abs/2201.01189) [cs.MS]
59. W. R. Inc. Mathematica, Version 12.3.1. (Champaign, 2021)
60. R. Hattori, N. Takayama, The singular locus of Lauricella’s FC. J. Math. S. Jpn. **66**(3), 981–995 (2014)

Springer Nature or its licensor (e.g. a society or other partner) holds exclusive rights to this article under a publishing agreement with the author(s) or other rightsholder(s); author self-archiving of the accepted manuscript version of this article is solely governed by the terms of such publishing agreement and applicable law.